archives
of thermodynamics
Vol. **37**(2016), No. 2, 107–120
DOI: 10.1515/aoter-2016-0015

Numerical analysis of the steam flow field in shell and tube heat exchanger

JAROSŁAW BARTOSZEWICZ*
LEON BOGUSŁAWSKI

Poznań University of Technology, Chair of Thermal Engineering, M. Sklodowskiej-Curie 5, 60-965 Poznań, Poland

Abstract In the paper, the results of numerical simulations of the steam flow in a shell and tube heat exchanger are presented. The efficiency of different models of turbulence was tested. In numerical calculations the following turbulence models were used: k-ε, RNG k-ε, Wilcox k-ω, Chen-Kim k-ε, and Lam-Bremhorst k-ε. Numerical analysis of the steam flow was carried out assuming that the flow at the inlet section of the heat exchanger were divided into three parts. The angle of steam flow at inlet section was determined individually in order to obtain the best configuration of entry vanes and hence improve the heat exchanger construction. Results of numerical studies were verified experimentally for a real heat exchanger. The modification of the inlet flow direction according to theoretical considerations causes the increase of thermal power of a heat exchanger of about 14%.

Keywords: Heat transfer; Heat exchanger; Shell and tube heat exchanger

Nomenclature

C	–	empirical constant
D	–	diameter, m
g	–	gravitational acceleration, m/s^2
i	–	phase number
k	–	kinetic energy of turbulence, m^2/s^2

*Corresponding Author. E-mail: jaroslaw.bartoszewicz@put.poznan.pl

L	–	length, m
p	–	pressure, Pa
P	–	power of heat exchanger, W
Pr	–	Prandtl number
r	–	volume fraction
R	–	empirical constant
Re	–	Reynolds number
Re_T	–	turbulent Reynolds number
S	–	additional source term
t	–	time, s
T	–	temperature, K
U	–	axis component of velocity, m/s
u	–	average velocity in the time measurement or calculation
V	–	radial component of velocity, m/s
x	–	coordinate of locations, m
y	–	coordinate of locations, m
Y	–	distance to the nearest wall, m

Greek symbols

α	–	angle of outflow, deg
ε	–	dissipation rate of turbulence, $\mathrm{m}^2/\mathrm{s}^3$
ν	–	kinematic viscosity, m^2/s
ρ	–	density, kg/m^3
τ	–	shear stress, Pa
ω	–	frequency of turbulence, 1/s

1 Introduction

In the paper, numerical simulations of a steam flow in a shell and tube heat exchanger are presented. The geometry of the analyzed heat exchanger PWC 630 [1] is shown in Fig. 1. This is a typical construction produced in Poland and used as a condenser in municipal power stations. Workshop studies, as far as corrosion and organic substances distribution are concerned, indicated that thermal loading of a heat transfer surface is not uniform. The inspection of the pipe surface quality near its ends indicated that thermal loading in this region of heat exchanger was very low. Basing on this observation, made during renovation, a numerical analysis of steam flow was carried out to obtain a possibility of improving steam flow by modifying flow direction at the inlet section of the heat exchanger. The numerical analysis of steam flow for different inlet flow directions was also carried out to obtain more uniform flow field.

Many papers are published in the world's literature every year on heat exchangers and their acting. This is the consequence of the extremely high

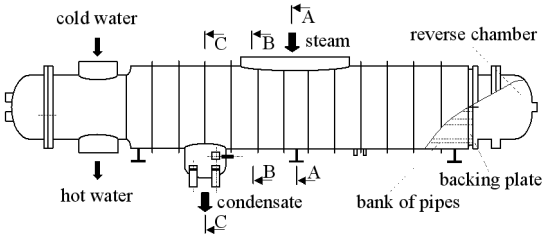

Figure 1: Raw view of a PWC630 [1] shell and tube heat exchanger with the indicated control section.

demand for experimental test results and numerical simulations covering technical cases of the occurrence of heat exchangers. Khaled *et al.* [4], Tang *et al.* [13] and Xie *et al.* [16] have conducted analytical and experimental investigations in the air heat exchanger. In the papers due to Wang *et al.* [14] and Liu *et al.* [9] have been presented the results including measurement of fin-and-tube heat exchangers with a larger diameter tube. Guo *et al.* [3] have shown the equivalent thermal resistance and the relationship between effectiveness and thermal resistance. All this papers include experimental and numerical analysis, concerning heat exchangers used in industries.

Calculations of steam flow around condenser pipes including phase changing are very complicated. Modern numerical codes give a possibility to predict the turbulent flow. This information can be used to improve the process of designing a heat exchanger. Numerical analysis of the flow in such complicated geometry give the possibility to predict the steam flow in order to uniformize the flow field in the heat exchanger. This ought to cause the increase of thermal loading of the heat exchanger surface. As a result of such a modification of the flow, it is possible to observe a rise in heat power of the heat exchanger and reduction of temperature gradients along pipes, which influences durability of pipes and risk of damage while operating.

2 Method of numerical analysis

The results of numerical analysis were obtained by applying the Phoenics software developed by CHAM Ltd. [11]. The differential equations of

transport of physical value φ can be expressed in the general form

$$\frac{d\,(r_i\rho_i\varphi_i)}{dt} + \mathrm{div}\left[r_i\rho_i u_i\varphi_i - r_i G_{\varphi i}\mathrm{grad}(\varphi_i)\right] = r_i S_{\varphi i}\ , \tag{1}$$

where φ is the dependent variable such as enthalpy, momentum per unit mass, turbulence energy, etc. Special expressions also have to be introduced for G and S, accounting for the correlations between velocity, density, φ and other properties of the flow and of the fluid. Subscript i in Eq. (1) shows the ability to perform the calculation for a multiphase flow. The case of single-phase flow was examined. The numerical analysis of the flow was conducted using Phoenics 3.3 code. The code used solver of transport equation in a uniform form [11]. Additionally, it was possible to use a two-equation model of turbulence for turbulent flows. In numerical calculations the following turbulence models were tested: k-ε, RNG k-ε, k-ω proposed by Wilcox, k-ε by Chen and Kim, and k-ε by Lam and Bremhorst.

2.1 The standard k-ε turbulence model

Software Phoenics provides the standard high Reynolds number form of the k-ε model, as presented by Launder and Spalding [7], and Launder *et al.* [8] which is as follows:

$$\frac{d\,(\rho k)}{dt} + \frac{d}{dx_i}\left[\rho U k - \frac{\rho\nu_t}{\mathrm{Pr}(k)}\frac{dk}{dx_i}\right] = \rho(P_k + G - \varepsilon)\ , \tag{2}$$

$$\frac{d\,(\rho\varepsilon)}{dt} + \frac{d}{dx_i}\left[\rho U_i\varepsilon - \frac{\rho\nu_t}{\mathrm{Pr}(\varepsilon)}\frac{d\varepsilon}{dx_i}\right] = \rho\frac{\varepsilon}{k}(C_1 P_k + C_3 G - C_2\varepsilon)\ , \tag{3}$$

where

$$\nu_t = C_M\frac{k^2}{\varepsilon}\ . \tag{4}$$

Empirical constants of turbulence model are $\mathrm{Pr}(k) = 1.0$, $\mathrm{Pr}(\varepsilon) = 1.314$, $C_M = 0.09$, $C_1 = 1.44$, $C_2 = 1.92$, $C_3 = 1.0$. P_k is a volumetric production rate of the kinetic energy of turbulence by shear forces and G is a volumetric production rate of the kinetic energy of turbulence by gravitational forces.

2.2 The k-ω turbulence model

The first two-equation turbulence model was Kolmogorov k-ω model [5]. However the k-ω model proposed by Wilcox [15] was used in the Phoenics program. This model is very often used in turbulence flow for a low

Reynolds number at the wall. The empirical constants are $\mathrm{Pr}(k) = 2.0$, $\mathrm{Pr}(f) = 2.0$. The damping functions, which are set to unity in the high Reynolds number model, are defined by

$$F_M = \frac{\frac{1}{40} + \frac{R_T}{R_K}}{1 + \frac{R_T}{R_K}}, \quad F_1 = \frac{\frac{1}{10} + \frac{R_T}{R_W}}{F_M\left(1 + \frac{R_T}{R_W}\right)}, \quad F_2 = \frac{\frac{5}{18} + \frac{R_T^4}{R_B^4}}{1 + \frac{R_T^4}{R_B^4}},$$

where $R_B = 8$, $R_K = 6$, $\mathrm{R}_W = 2.7$ and $R_T = k/(f\nu)$.

2.3 RNG *k-ε* turbulence model

Yakhot and Orszag [17] described the k-ε model based on the renormalization group (RNG) methods. In this approach the RNG techniques are used to develop a theory for a large scale vortex in which the effects of small scales vortex are represented by modified transport coefficients. The RNG k-ε model differs from the standard high Reynolds number form of k-ε model in empirical constants: $\mathrm{Pr}(k) = 0.7194$, $\mathrm{Pr}(\varepsilon) = 0.7194$, $C_1 = 1.42$, $C_2 = 1.68$, $C_3 = 1.0$, $C_M = 0.0845$ [18].

2.4 *k-ε* turbulence model modified by Chen-Kim

The standard high Reynolds number form of the two-equation k-ε turbulence model employs a single time scale k/ε to characterize various dynamic processes occurring in turbulent flows. Chen and Kim [2] proposed a modification, which improves the dynamic response of the equation for ε by introducing the additional time scale k/P_k, where P_k is the volumetric production rate of k. The Chen-Kim model differs from the standard high Reynolds form of the k-ε model in empirical constants $\mathrm{Pr}(k) = 0.75$, $\mathrm{Pr}(\varepsilon) = 1.15$, $C_1 = 1.15$, $C_2 = 1.9$, and the additional timescale k/P_k is included in the ε-equation via the following additional source term per unit of volume

$$\frac{dS}{d\varepsilon} = \rho F_1 C_3 \frac{P_k^2}{k}, \tag{5}$$

where $C_3 = 0.25$ and C_1 is the Lam-Bremhorst damping function which tends to unity at high turbulence Reynolds numbers.

2.5 Lam-Bremhorst *k-ε* turbulence model

In the Lam-Bremhorst k-ε turbulence model, the transport equation for the total dissipation rate was used [6]. This model solves fluxes for low

Reynolds number. The form of the model implemented in Phoenics was described by Patel *et al.* [10]. The Lam-Bremhorst low Reynolds number k-ε model differs from the standard high Reynolds number model by the fact that empirical coefficients C_M, C_1 and C_2 are multiplied by the functions

$$F_M = \left(1 - e^{-0.0165\mathrm{Re}}\right)^2 \left(1+\frac{20.5}{\mathrm{Re}_T}\right) , \quad F_1 = 1+\left(\frac{0.05}{F_M}\right)^3 , \quad F_2 = 1-e^{-\mathrm{Re}_T{}^2} ,$$

where $\mathrm{Re} = \frac{Y\sqrt{k}}{\nu}$ and $\mathrm{Re}_T = \frac{k^2}{Y\varepsilon}$.

3 Boundary conditions

A numerical analysis of the flow was carried out assuming that the flow inlet section of the heat exchanger has to be divided into three parts as it is shown in Fig 2. The angle of steam flow was determined individually for each zone of the inlet section to obtain the best configuration of the entry vanes and optimise the heat exchanger construction, taking into account the uniform flow field around the heat exchange surface. The numerical analysis was performed not taking into account the condensation with the isothermal walls of the bank of pipe. The temperature of the surface was assumed as equal to one degree above the temperature of condensation. This simplification was due to the imposed deadlines for implementation of the work. Most important, from the point of view of the customer, was information about the mass distributions along the top part of the pipe bank. These mass redistributions section below have a small effect. For numerical calculations in the region between inlet section of heat exchanger and first row of pipes the uniform grid was used.

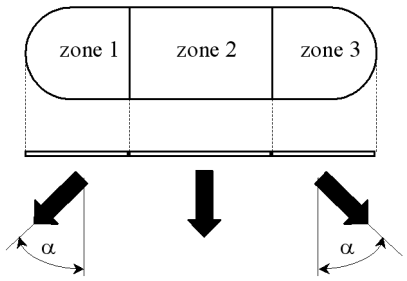

Figure 2: Scheme of the steam inlet section divided into three zones.

The analysed heat exchanger, which is shown in Fig. 1, was made of 5196

copper pipes. Each of these pipes had a diameter of 0.02 m, thickness of 0.001 m, and length of 9.066 m. The internal diameter of the heat exchanger was 2.22 m. The fluid flux of hot municipal water varied from 525 to 700 kg/s, and the temperature in the inlet ranged from 303 to 363 K. The steam, which supplied in the heat exchanger, had the temperature of 393 K, and the overpressure ranged from 0.016 to 0.32 MPa. The mass flow rate of steam was 52.8 kg/s.

Figure 3 shows characteristic surfaces of the heat exchanger, for which the average value of velocity was calculated. There are three vertical surfaces (A,B,C), five horizontal ones (I–V) and one vertical 'norm surfaces', which is cutting off the shell and the tube heat exchanger zone to two equal parts.

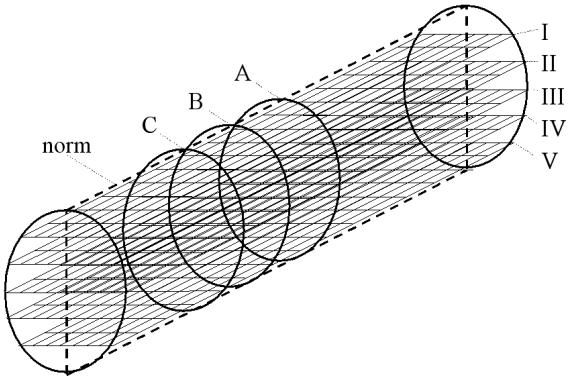

Figure 3: Localization of control surfaces inside the heat exchanger.

4 Numerical results and discussion

The chosen results of numerical calculations for steam flow in the shell and tube heat exchanger are presented in the figures, which show distribution on normal surfaces ('norm') for values, that were used as the average ones for surfaces from I to V. Figure 4 shows the location of maximum velocity in the analysed profiles for five two-equation turbulence models used in the calculations. The differences between the results are very small within the limits of measurement errors. The axis of abscissa was the ratio of the location to the length of pipes, L, and the axis of ordinates was the ratio of the location to the diameter of the heat exchanger, D, in percentage. In Fig. 5 the distributions of average velocity for five turbulence models are

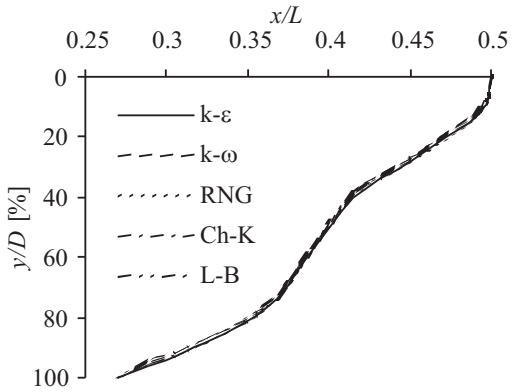

Figure 4: Location of maximum velocity of the steam flow in the heat exchanger obtained using the following five turbulence models: k-ε for high Reynolds number, Wilcox k-ω, Ch-K – Chen-Kim k-ε , L-B – Lam-Bremhorst k-ε, RNG – k-ε proposed by Yakhot and Orszag.

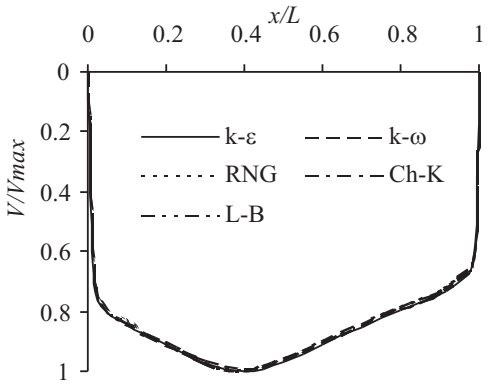

Figure 5: Distribution of mean velocity on control surface no. III for five turbulence models.

presented. The velocity (V) was normalized by the maximum value of velocity (V_{max}). The velocity profiles obtained using five different turbulence models are practically the same, therefore all the adopted models can be used for heat exchanger analysis.

The computed distribution of velocity field in the heat exchanger for a determined flow direction at the inlet section is presented in Fig. 6. The flow fields in cross-section for three chosen sections according to the local-

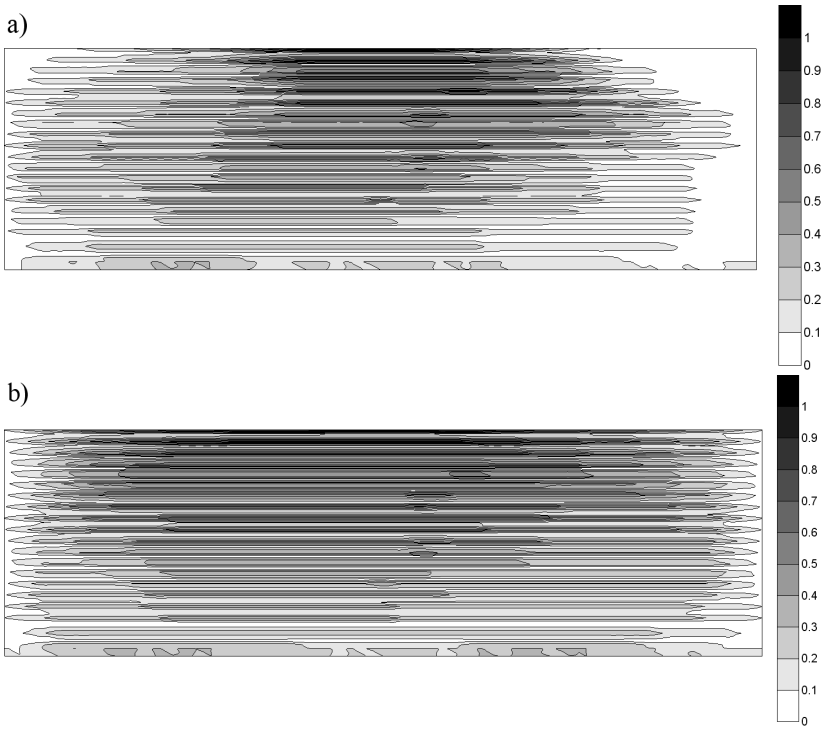

Figure 6: Isolines of velocity normalized by the maximum value of velocity on the 'norm surface' for: a) left angle outlet 5° and right angle outlet 0°; b) left angle outlet 15° and right angle outlet 15°.

ization in Fig. 3 are presented in Fig. 7. The analysis of many configurations of the flow at the inlet of the heat exchanger was conducted.

Figures from 8 to 10 illustrated the results of numerical calculations for three horizontal surfaces for the k-ε turbulence model proposed by Launder and Spalding [7]. These plots show the radial component of the velocity (V) normalized by the maximum value of velocity (V_{max}) on the analysed surfaces. The profiles of the velocity depend on the angles of the steam outflow from the inlet sections.

When the angle of the outflow flow at the inlet section was 0° the jet of steam flows to the central part of the heat exchanger and the side parts of the heat exchanger were not supplied with the fresh water vapor. Distribution of velocity was strongly nonuniform and the exchanging heat flux was minimal. When the angle of the outflow was bigger than 15° then the profile of average velocity was also nonuniform. The jet flow along the

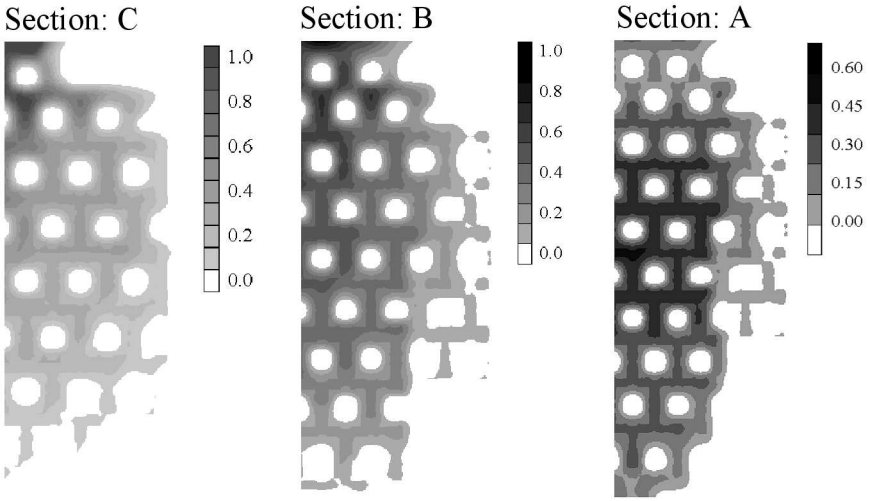

Figure 7: The part of field of relative velocity in heat exchanger for the characteristic cross-section which are shown in Fig. 1 at: zone 1 $\alpha = 0°$, zone 2 $\alpha = 0°$ and zone 3 $\alpha = 0°$.

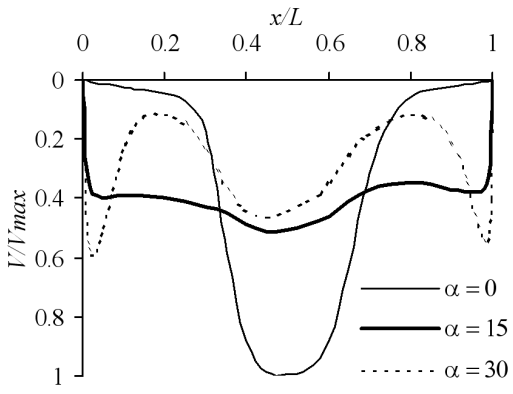

Figure 8: Distribution of mean velocity on control surface no. I for three angles, α, of the outflow.

perforated buttons and power of the heat exchanger diminished. The best results were obtained when the angle of the outflow was about 15°. In this case, distribution of velocity was most uniform in the whole heat exchanger.

The fundamental aim of these studies is to obtain a uniform distribution of velocity, which gives uniform distribution of mass flow rate in the heat

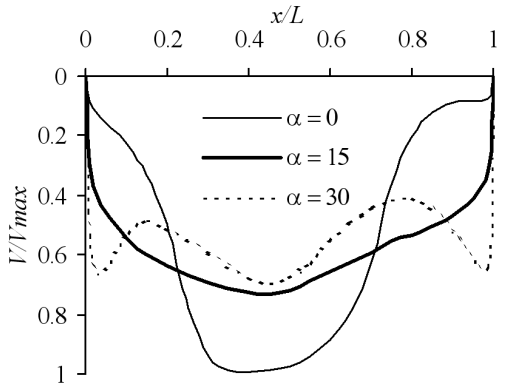

Figure 9: Distribution of mean velocity on the control surface no. III for three angles, α, of the outflow.

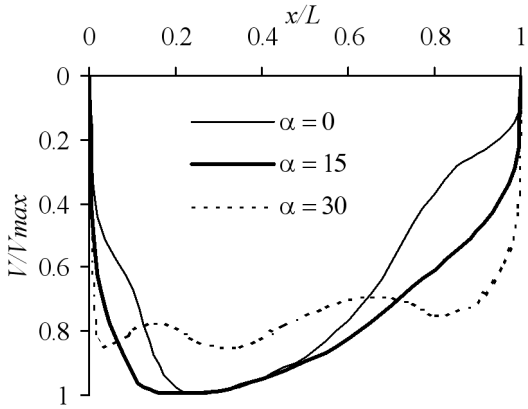

Figure 10: Distribution of mean velocity on the control surface no. V for three angles, α, of the outflow.

exchanger. More uniform steam mass flow around pipe surface results in the increase of heat power of the heat exchanger.

5 Experimental verification of numerical simulations results

During many years of operating of two heat exchangers PWC 630 it was never noticed to attain the value of power offered by the producer. The

nominal value was confirmed by authors calculations and was of about 250 MW. The real, maximal power of the analysed heat exchangers recorded by power station staff was of about 210 MW. Numerical simulations indicated that for the used inlet configuration, heat exchanger did not work effectively because of a nonuniform flow around the pipe bed. The modification of inlet section was done according to the results of numerical calculations. The inlet section was modified to obtain the angles of $-15°$, $0°$, $15°$ for which the most uniform flow over heat exchanger was obtained in numerical simulations.

New thermal characteristics of heat transfer after modernization of the inlet section are shown in Fig. 11. Measurements of heating power were carried for a period of three months of the heating season with the use of the measurement system of the power station. Figure shows two plots of thermal power at two different mass flow rate of water for different temperatures at the inlet to the heat exchanger. The results relate to the measurement of the heating season in 2008 and 2009. The study was done on the basis of the measuring instruments mounted on the installation in the plant. Data from Fig. 11 should be treated only as the utilities data.

The test of exchangers after modernization indicated the increase of maximal thermal power up to 240 MW with about 2.3% error (an estimate based on the data provided by the staff of the plant). The numerical simulation of the flow in a heat exchanger gives a possibility to improve its performance and increase thermal power of heat exchanger by 14%. This noticeable effect was possible to obtain thanks to a relatively simple modification of the inlet section of the heat exchanger.

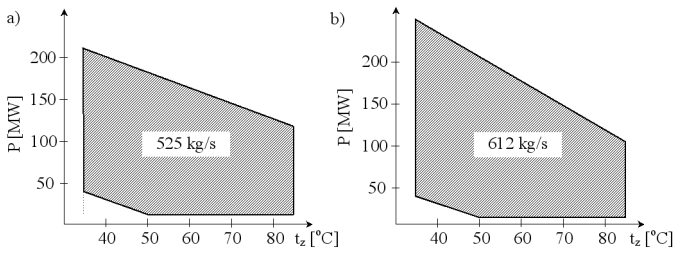

Figure 11: Results of experimental tests of the heat exchanger after modernization of the inlet section; the thermal power versus temperature for two different mass flow rate of water: a) 528 kg/s; b) 612 kg/s.

6 Conclusions

Numerical analysis of steam flow in the heat exchanger, that is used at the municipal power station in Poznan was presented. The effectiveness of five two-equation turbulence models was tested. The results of the numerical simulations were similar. Differences between the velocity values for the turbulence model k-ε, RNG k-ε, Wilcox k-ω, Chen-Kim k-ε , and the Lam-Bremhorst k-ε were very small. The effect of the change of the angle in the heat exchanger inlet section was analysed, because of limited possibilities of modifying of geometries of the heat exchanger installed in power station. Calculations for different inflow angles at the inlet were performed to obtain the most uniform steam flow in the heat exchanger, which was used as the simplest indicator to estimate the effectivity of heat transfer. The most uniform flow was obtained for the inlet flow slitted on three jet at the angles $-15°$, $0°$, and $15°$. For these conditions, distribution of velocity was the most uniform in the whole heat exchanger. It was assumed that when the velocity field is uniform, then the steam mass flow rate is also uniform and the thermal power of the heat exchanger takes the maximum value. According to the numerical study modernization of the inlet section of heat exchanger was carried out using the theoretically optimised value of the inlet angle. Experimental tests of the heat exchanger after modernization indicated about 14% increase of the maximum thermal power from 210 to 240 MW. The results of numerical studies were applied and a new shell and tube heat exchanger with the improved inlet section is now in use in municipal power station.

Received in February 2012, in revised form in March 2016

References

[1] Bartoszewicz J.: *Heat exchangers PWC 630 – 2800 – 16/25V – B*. Report of Power Station Technical Service, Poznań 2001 (in Polish).

[2] Chen Y.S., Kim S.W.: *Computation of turbulent flows using an extended k-ε turbulence closure model*. NASA CR-179204, 1987.

[3] Guo Z.Y., Liu X.B., Tao W.Q., Shah R.K.: *Effectiveness-thermal resistance method for heat exchanger design and analysis*. Int. J. Heat Mass Transfer **53**(2010), 13-14, 2877–2884.

[4] Khaled M., Harambat F., Peerhossini H.: *Analytical and empirical determination of thermal performance of louvered heat exchanger – Effects of air flow statistics*. Int. J. Heat Mass Transfer **54**(2011), 1-3, 356–365.

[5] Kolmogorov A.N.: *Equations of turbulent motion of incompressible fluid* . Izv. Akad. Nauk SSR, Ser. Phys. **6**(1942), 1/2, 56.

[6] Lam C.K.G., Bremhorst K.: *A modified form of the k-ε model for predicting wall turbulence*. Trans. ASME J. Fluids Eng. **103**(1981), 456–460.

[7] Launder B.E., Spalding D.B.: *The numerical computation of turbulent flows*. Comp. Mech. Appl. Mech. Eng. **3**(1974), 269-289.

[8] Launder B.E., Spalding D.B., Rodi W.: *Progress in the development of a Reynolds stress turbulence closure*. J. Fluid Mech. **68**(1975), 537.

[9] Liu Y.C., Wongwieses S., Wang Q.W.: *Airside performance of fin-and-tube heat exchangers in dehumidifying conditions – data with larger diameter*. Int. J. Heat Mass Transfer **53**(2010), 7-8, 1603–1608.

[10] Patel V.C., Rodi W., Scheurer G.,: T*urbulence models for near-wall and low-Reynolds-number flows: A review*. AIAA J. **23**(1984), 9, 1308–1319.

[11] Rosten H.I., Spalding D.B.: *The PHOENICS beginners guides*. CHAM Report, No. TR100, CHAM Ltd., Wimbledon 1985.

[12] Spalding D.B.: *Mathematical models of turbulent transport processes*. HTS/79/2, Imperial Collage, Mech. Eng. Dept., London 1979.

[13] Tang L.H., Zeng M., Wang Q.W.: *Experimental and numerical investigation on air-side performance of fin-and-tube heat exchangers with various fin patterns*. Exp. Therm. Fluid Sci. **33**(2009), 818–827.

[14] Wang C.C., Liaw J.S., Yang B.C.: *Airside performance of herringbone wavy fin-and-tube heat exchangers – data with larger diameter tube*. Int. J. Heat Mass Transfer **54**(2011), 5-6, 1024–1029.

[15] Wilcox D. C.: *Reassessment of the scale determining equation for advanced turbulence models*. AIAA J. **26**(1988), 11, 1299–1310.

[16] Xie G., Wang Q., Sunden B.: *Parametric study and multiple correlations on air-side heat transfer and friction characteristics of fin-and-tube heat exchangers with large number of large-diameter tube rows*. Appl. Therm. Eng.**29(**2009), 1–16.

[17] Yakhot V., Orszag S.A.: *RNG analysis of turbulence*. J. Sci. Comput. **1**(1986), 3–51.

[18] Yakhot V., Smith S.A.: *The renormalization group, the eps-expansion and derivation of turbulence models*. J. Sci. Comput. **7**(1992), 35–61.